ARTICLE

Investigation on Exciton Relaxation Kinetics of ZnCuInS/ZnSe/ZnS Quantum Dots by Time-Resolved Spectroscopy Techniques

Xue-cong Li[a*], Ning Sui[b], Yu Zhang[c*]

a. Department of Physics, Tianjin Polytechnic University, Tianjin 300387, China
b. College of Physics, Jilin University, Changchun 130012, China
c. State Key Laboratory on Integrated Optoelectronics, College of Electronic Science and Engineering, Jilin University, Changchun 130012, China

(Dated: Received on September 8, 2014; Accepted on November 16, 2014)

The exciton relaxation kinetics of ZnCuInS/ZnSe/ZnS quantum dots (QDs) is investigated by time-resolved spectroscopy techniques in detail. Based on the rate distribution model, the wavelength-dependent emission dynamics shows that the intrinsic exciton, the exciton in the interface defect state and that in donor-acceptor pair state (DAPS) together participate in the photoluminescence process of QDs, and the whole emission process is mainly dependent on the DAPS emission. Transient absorption data show that the intrinsic exciton and the interface defect species maybe together appear after excitation and the intensity-dependent Auger recombination process also exists in QDs at high excitation intensity.

Key words: Quantum dots, Time-resolved spectroscopy, Exciton relaxation kinetics

I. INTRODUCTION

Colloidal inorganic quantum dots (QDs) have received considerable attention because of their interesting optical properties and potential application in the fields of light-emitting diode [1, 2], optical gain media [3, 4], and solar-harvesting [5, 6]. Recently, a new kind of I-III-VI nano-materials such as $CuInS_2$ [7, 8] and ZnCuInS [9, 10], has attracted much attention, due to its low toxicity, large absorption coefficient, and size-tunable emissions [7−11]. These QDs have exhibited highly efficient and widely tunable photoluminescence (PL) from visible to the NIR region by varying not only the size but also the composition in nano-particles. An important strategy to improve the QD's PL efficiency and stability is to overgrow a semiconductor shell structure with a wider band-gap around the QDs, resulting in the so-called type I core/shell systems, such as ZnCuInS/ZnS [9] and ZnCuInS/ZnSe/ZnS QDs [12, 13]. For this type of QDs, the ZnS (3.7 eV) shell structure can protect the internal structures from the solvent environment and simultaneously obviate exciton dissociation. However, the report on the exciton relaxation process occurring in this new kind of QDs is much limited, which could hinder their development and utilization in the optoelectronic devices.

In this work, we probed the exciton relaxation process of ZnCuInS/ZnSe/ZnS core/shell/shell QDs by using femtosecond transient absorption (TA) and picosecond time-correlated single-photon counting (TCSPC) techniques. The emission wavelength-dependent dynamic behaviors show that multiple luminescent species, involving the intrinsic exciton, the exciton in the interface defect state (IDS) and that in donor-acceptor pair state (DAPS), together participate in the PL process. The time-resolved TA measurement further confirms that multiple exaction states appear after photoexcitation and the intensity-dependent Auger recombination (AR) process also occurs at high excitation intensity.

II. EXPERIMENTS

The synthesis of ZnCuInS/ZnSe/ZnS QDs was described in Ref.[11]. The images of the particles were taken using a JEOL FasTEM-2010 transmission electron microscope (TEM) and exhibited that the diameter of QDs was ∼2.7 nm. TCSPC measurement was performed by a fluorescence spectrometer (mini-τ, Edinburgh Photonics) equipped with an EPL405 laser diode. Femtosecond Titanium: Sapphire laser (Coherent) was used as a radiation source, which offered 2.2 mJ, 130 fs pulses at 800 nm with a repetition rate of 1 kHz. The PL measurements were achieved using a fiber optic spectrometer (Ocean Optics, USB4000). The detailed setup of femtosecond TA measurement can be found in Ref.[14]. The excitation wavelength was 400 nm in the TA experiment. All the measurements were performed at room temperature.

*Authors to whom correspondence should be addressed. E-mail: lixcyy@163.com, yuzhang@jlu.edu.cn

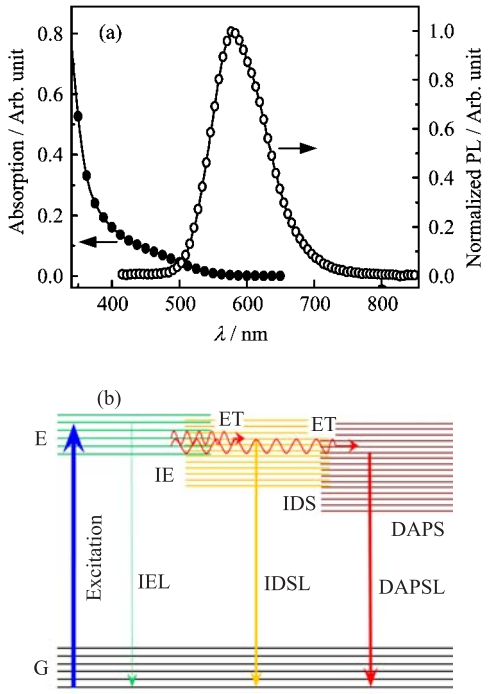

FIG. 1 (a) UV-Vis absorption and photoluminescence spectra of ZnCuInS/ZnSe/ZnS QDs. (b) Proposed luminescence mechanism in ZnCuInS/ZnSe/ZnS QDs. IE: intrinsic exciton, IEL: intrinsic exciton luminescence, IDSL: the interface defect state luminescence, DAPSL: the donor-acceptor pair state luminescence, ET: energy transfer; E: excited state; G: ground state.

III. RESULTS AND DISCUSSION

UV-Vis absorption and normalized PL spectra of ZnCuInS/ZnSe/ZnS QDs are shown in Fig.1(a). Although the absorption spectrum of the QDs is almost structureless, the first excitation band at the absorption edge is still observed, which is consistent with a previously reported result [13]. The absorption band edge of QDs is located at ∼553 nm. The emission peak of QDs is ∼580 nm, and the corresponding full width at half-maximum (FWHM) is ∼94 nm, which is significantly broader than those of high-quality CdSe QDs [15], but similar to the CuInSe QDs [16], indicating that the luminescence from donor-acceptor pairs (created by defects and vacancies) recombination [9] may play an important role in the PL spectrum of this QDs. According to the previous report [9], multiple transient luminescent species appear after photoexcitation, as seen in Fig.1(b), which are composed of intrinsic exction, interface exciton state and donor-acceptor pair state, and they together participate in the PL process of QDs.

In order to understand the photophysical property of these transient species through the photoluminescence characteristics, the time-dependent emission spectra of ZnCuInS/ZnSe/ZnS QDs are given in Fig.2(a), which exhibits that the emission maximum shows a little red-

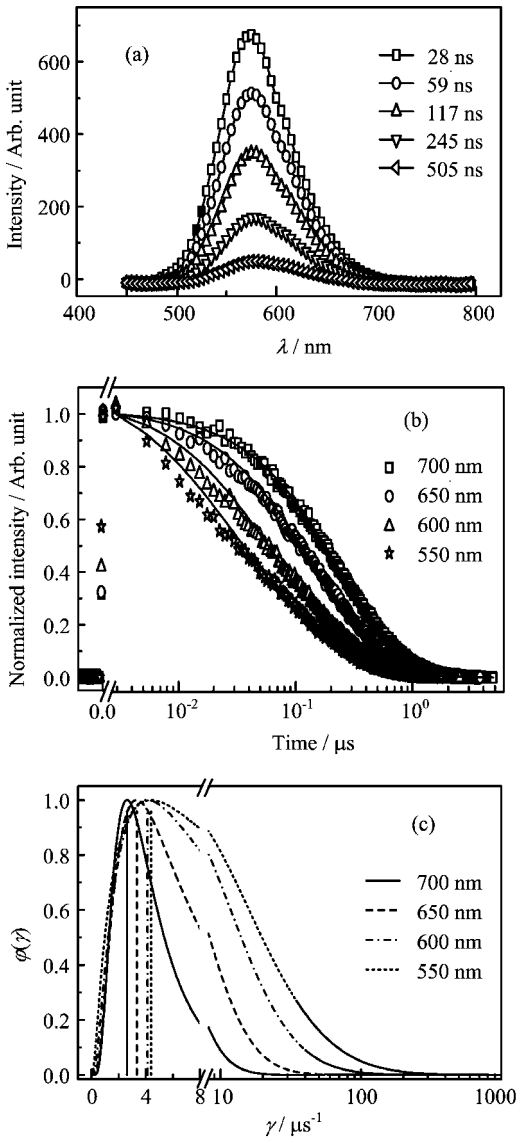

FIG. 2 (a) The temporal emission spectra of quantum dots. (b) Wavelength-dependent emission curves. (c) The decay-rate distributions $\varphi(\gamma)$ at different wavelengths. γ_{MF} of emission traces at 550, 600, 650, and 700 nm are 4.39, 4.13, 3.33, and 2.62 μs^{-1}, and the widths ($\Delta\gamma$) of their distribution function are 26.00, 16.97, 8.94, and 5.10 μs^{-1}.

shift over time. Apparently, these transient species could together appear in the emission spectrum at 28 ns. With the time prolonging, some of transient species could disappear. In the emission spectrum at 505 ns, the component originated from intrinsic exciton could annihilate, which could be responsible for the redshifting of emission spectrum. Therefore, these transient species have difference in emission spectrum, but are not obvious. It suggests that the emission spectra of these transient species are all broad. The wavelength-dependent emission curves of QDs are shown in Fig.2(b), so as to compare the relaxation rates

DOI:10.1063/1674-0068/28/cjcp1409143

among these transient species. It shows that all emission traces strongly deviate from a single-exponential decay and the relaxation rate becomes slow with the redshifting of the emission wavelength. To explain this phenomenon, three reasons could be provided as follows: (i) multi-type luminescent species participate in the emission relaxation process [17−19] and their relaxation rates have difference, which leads to the non-exponential relaxation behavior; (ii) the weight of transient species in emission traces varies with the emission wavelength, due to the difference among their emission spectra; (iii) the relaxation rates of these transient species may have a distribution width in rate region, since their emission spectra are all broad. The total emission traces could not show a single-exponential relaxation behavior. Therefore, all the emission traces are fitted with a continuous distribution function of decay rates [20] due to the overlapping in decay rate γ:

$$I(t) = I(0) \int_{\gamma=0}^{\infty} \varphi(\gamma) \exp(-\gamma t)\, \mathrm{d}\gamma \tag{1}$$

where $\varphi(\gamma)$ is a distribution of decay rates with dimension of time, $I(0)$ is the initial intensity of signal, $\varphi(\gamma)$ describes a distribution of the concentration of transient species with a certain γ, weighted by the corresponding γ_{rad} [21]. $\varphi(\gamma)$ is the distribution function as described:

$$\varphi(\gamma) = A \exp\left[-\ln^2\left(\frac{\gamma}{\gamma_{\mathrm{MF}}}\right)\frac{1}{w^2}\right] \tag{2}$$

where γ_{MF} is the most-frequency decay rate corresponding to the maximum of $\varphi(t)$, w is a dimensionless width parameter that determines the distribution width ($\Delta\gamma$) at 1/e, A is thenormalization constant, so that

$$\int \varphi(\gamma)\mathrm{d}\gamma = 1 \tag{3}$$

γ_{MF} is determined by the decay rates which are dependent on the situation of the transient species. Meanwhile, the distribution width $\Delta\gamma$ could be calculated as,

$$\Delta\gamma = 2\gamma_{\mathrm{MF}} \sinh w \tag{4}$$

As seen in Fig.2(c), γ_{MF} and $\Delta\gamma$ could increase as the emission wavelength increases. As mentioned above, multi-transient species, involving the intrinsic exciton [19], interfacedefect state and donor-acceptor pair state [17], participate in the photoluminescence process, the $\Delta\gamma$ should be broad. Due to the difference among their emission spectra, the γ_{MF} should depend on the emission wavelength. It is accepted that among them the relaxation rate of the intrinsic exciton is the fastest and that of donor-acceptor pair state (DAPS) is the slowest. Therefore, the γ_{MF} also gradually decelerates from 4.39 μs^{-1} to 2.62 μs^{-1}, when the emission wavelength red shifts from 500 nm to 700 nm. Meanwhile, the $\Delta\gamma$ at 550 nm is broader than that at 700 nm, which is due to the disappearance of intrinsic exciton at long emission wavelength region. In a word, the transient species in QDs all have a broad emission spectrum and a broad rate distribution, which lead to a broad emission spectrum and a complex emission dynamics.

Note the weight of transient luminescent species with high radiative rate, which corresponds to the IE, apparently decreases (as seen in Fig.2(c)), as the emission wavelength blue shifts, indicating that the IE is mainly distributed on the high energy state (as seen in Fig.1(b)). The transient luminescent species with low radiative rate (<4 μs^{-1}) has a broad energy distribution and all the emission wavelengths own their component, indicating that this transient species should correspond to the DAPS. In addition, the γ_{MF} in different emission traces is mainly distributed at the low rate region (<4 μs^{-1}), indicating that the DAPS emission plays an important role in the whole emission mechanism.

As seen in Fig.3 (a) and (b), TA spectra of QDs are performed and composed of negative spectral bands, which may correspond to the ground state bleaching (GSB) and simulated emission (SE) respectively, and two parts of positive absorption bands correspond to the excited state absorption (EA) peaks at ∼625 and ∼800 nm, respectively. The positive signal at 760 nm decreased quickly in comparison with that of the negative band at 550 nm at the initial time, and then became slow after ∼20 ps. The TA spectra at 553 ps show that the negative spectral signal disappears, and the EA features at 625 and 800 nm still exist. A valley appears between the EA peaks at 625 and 800 nm in the TA spectrum at 1 ps and should be assigned to the stimulated emission (SE), since its position is consistent with that of the steady emission band. It suggests that the SE signal is covered by EA at long time scale. The normalized decay curves of EA and GSB are shown in Fig.3(b). An obvious fast decay component appears in the EA curve (at ∼760 nm) and the rate of GSB would exceed that of EA after 175 ps. The difference between them should be assigned to the appearance of multiple transient species. Besides the IE, the IDS and DAPS maybe appear through cascade energy transferring.

In order to further understand the exciton relaxation, the intensity-dependent TA curves at 760 nm of QD are shown in Fig.3(c). Herein, a fast relaxation behavior appears in TA curves, which decays much faster and couldn't be assigned to the fast carrier interface trapping process. Meanwhile, its percentage in the TA curves gradually enhances as the excitation intensity increases, indicating that this intensity-dependent fast decay process should be attributed to the AR process [22]. The complexity of AR spurred researchers to develop several models to resolve its dynamic process [3, 23, 24]. Because TA curves at high intensity are the linear combinations of AR and single-exciton relaxation (SER) [22], we simplified the approach of the intensity-

DOI:10.1063/1674-0068/28/cjcp1409143

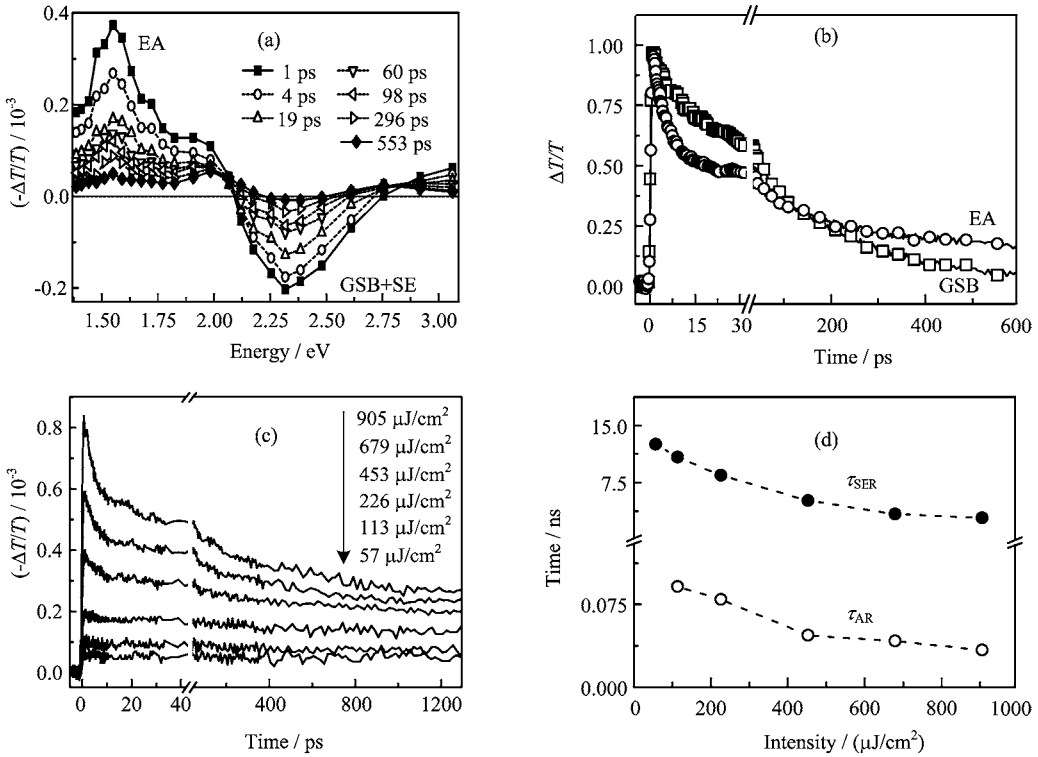

FIG. 3 (a) Transient absorption spectra of QDs at different time delay. (b) Kinetic traces at 1.63 and 2.25 eV after excitation at 400 nm laser light with intensity of 452.7 μJ/cm^2. (c) Kinetic traces at 760 and 550 nm after excitation at 400 nm laser light with intensity of 452.7 μJ/cm^2. (d) Intensity-dependent lifetime of single-exciton relaxation and Auger recombination processes.

dependent TA curves, and describe them as,

$$N_{\mathrm{QD}}(t) = N_{\mathrm{AR}}(t) + N_{\mathrm{SER}}(t) \tag{5}$$

$$N_{\mathrm{SER}}(t) = A_{\mathrm{SER}} \exp\left(\frac{-t}{\tau_{\mathrm{SER}}}\right) \tag{6}$$

$$N_{\mathrm{AR}}(t) = \sum_i A_{\mathrm{AR}\text{-}i} \exp\left(\frac{-t}{\tau_{\mathrm{AR}\text{-}i}}\right) \tag{7}$$

where $N_{\mathrm{SER}}(t)$ and $N_{\mathrm{AR}}(t)$ correspond to the number of exciton participating the single-exciton relaxation and AR process, respectively. $N_{\mathrm{SER}}(t)$ could be described by using a mono-exponential function, and A_{SER} represents the relative weight of single-exciton relaxation in the TA curves. $N_{\mathrm{AR}}(t)$ could be described by a bi-exponential function of high intensity, where $A_{\mathrm{AR}\text{-}i}$ represents the weight of lifetimes. Here, the total decay traces would be fitted by tri-exponential function, when the intensity is higher than 113.2 μJ/cm^2. The single-exciton dynamics would correspond to the longest lifetime (τ_{SER}). By subtracting the decay component of SE from the TA curves, the lifetime of AR (τ_{AR}) could be obtained according to the function

$$\tau_{\mathrm{AR}} = \frac{A_{\mathrm{AR}\text{-}1}\tau_{\mathrm{AR}\text{-}1} + A_{\mathrm{AR}\text{-}2}\tau_{\mathrm{AR}\text{-}2}}{A_{\mathrm{AR}\text{-}1} + A_{\mathrm{AR}\text{-}2}} \tag{8}$$

Figure 3(d) summarizes the τ_{AR} and τ_{SER} of QDs at different intensity and shows both τ_{SE} and τ_{SER} monotonously decrease with the increase of intensity. With the increasing of intensity, the AR process gradually accelerates. For the normal AR process insemiconductor QD [24], the τ_{AR} depends on the number of localized defect states, which could act as final acceptor states that Auger electron to transfer to. After Auger recombination, more and more excitons are left in defect states of QDs, which accelerate the final exciton relaxation.

IV. CONCLUSION

Time-resolved spectroscopy techniques were employed to investigate the exciton relaxation kinetics in ZnCuInS/ZnSe/ZnS QDs. Multiple luminescent species, involving the intrinsic exciton, the exciton in the interface defect state (IDS) and that in donor-acceptor pair state (DAPS), participate in the fluorescence relaxation process. Based on the rate distribution model, the DAPS with low radiative rate should play an important role in the whole luminescence process. In addition, the transient absorption data offered the exciton relaxation process of QDs in an ultrafast time region which exhibits that the IDS and DAPS maybe appear through cascade energy transferring after photoexcitation and the intensity-dependent AR still existed in QDs.

DOI:10.1063/1674-0068/28/cjcp1409143

V. ACKNOWLEDGMENTS

This work was supported by the National Natural Science Foundation of China (No.61106039) and Science & Technology Development Foundation of Tianjin Higher Education Institutions (No.20140904).

[1] V. L. Colvin, M. C. Schlamp, and A. P. Alivisatos, Nature **370**, 354 (1994).
[2] N. Tessler, V. Medveldev, M. Kazes, S. H. Kan, and U. Banin, Science **295**, 1506 (2002).
[3] S. Strauf, K. Hennessy, M. T. Rakher, Y. S. Choi, A. Badolato, L. C. Andreani, E. L. Hu, P. M. Petroff, and D. Bouwmeester, Phy. Rev. Lett. **96**, 127404 (2006).
[4] M. Kazes, D. Y. Lewis, T. Ebenstein, T. Mokari, and U. Banin, Adv. Mater. **14**, 317 (2002).
[5] I. Robel, V. Subramanian, M. Kuno, and P. V. J. Kamat, J. Am. Chem. Soc. **128**, 2385 (2006).
[6] P. V. J. Kamat, J. Phys. Chem. C **112**, 18737 (2008).
[7] H. Nakamura, W. Kato, M. Uehara, K. Nose, T. Omata, O. S. Matsuo, M. Miyazaki, and H. Maeda, Chem. Mater. **18**, 3330 (2006).
[8] H. Zhong, Y. Zhou, M. Ye, Y. He, J. Ye, C. He, and Y. Li, Chem. Mater. **20**, 6434 (2008).
[9] W. J. Zhang and X. H. Zhong, Inorg. Chem. **50**, 4065 (2011).
[10] L. D. Trizio, M. Prato, A. Genovese, A. Casu, M. Povia, R. Simonutti, M. J. P. Alcocer, C. D'Andrea, F. Tassone, and L. Manna, Chem. Mater. **24**, 2400 (2012).
[11] L. Li, T. J. Daou, I. Texier, T. T. K. Chi, N. Q. Liem, and P. Peiss, Chem. Mater. **21**, 2422 (2009).
[12] Z. N. Tan, Y. Zhang, C. Xie, H. P. Su, C. F. Zhang, N. Dellas, S. E. Mohney, Y. Q. Wang, J. K. Wang, and J. Xu, Adv. Mater. **23**, 3553 (2011).
[13] Y. Zhang, C. Xie, H. P. Su, J. Liu, S. Pickering, Y. Q. Wang, W. W. Yu, J. K. Wang, Y. D. Wang, J. Hahm, N. Dellas, S. E. Mohney, and J. Xu, Nano Lett. **11**, 329 (2011).
[14] Y. H. Wang, J. Q. Hou, Z. H. Kang, L. J. Gong, T. H. Huang, L. L. Qu, Y. G. Ma, R. Lu, and H. Z. Zhang, Chem. Phys. Lett. **566**, 17 (2013).
[15] S. Taguchi, M. Saruyama, T. Teranishi, and Y. Kanemitsu, Phys. Rev. B **83**, 155324 (2011).
[16] P. M. Allen and M. G. J. Bawend, J. Am. Chem. Soc. **130**, 9240 (2008).
[17] L. Li, A. Pandey, D. J. Werder, B. P. khanal, J. M. Pietryga, and V. I. Klimov, J. Am. Chem. Soc. **133**, 1179 (2011).
[18] J. Z. Zhang, Acc. Chem. Res. **30**, 423 (1997).
[19] F. Wu, J. Z. Zhang, R. Kho, and R. K. Mehra, Chem. Phys. Lett. **330**, 237 (2000).
[20] I. S. Nikolaev, P. Lodahl, A. F. van Driel, A. F. Koenderink, and W. L. Vos, Phys. Rev. B **75**, 115302 (2007).
[21] A. F. van Driel, I. S. Nikolaev, P. Vergeer, P. Lodahl, D. Vanmakekelbergh, and W. L. Vos, Phys. Rev. B **75**, 035329 (2007).
[22] V. I. Klimov, A. A. Mikhailovsky, D. W. McBranch, C. A. Leatherdale, and M. G. Bawendi, Science **287**, 1011 (2000).
[23] I. Robel, B. A. Bunker, P. V. Kamat, and M. Kuno, Nano. Lett. **6**, 1344 (2006).
[24] A. L. Efros and A. L. Efros, Sov. Phys. Semicond. **16**, 772 (1982).

DOI:10.1063/1674-0068/28/cjcp1409143